actuators

Article

Spiral Spring-Supported Force Plate with an External Eddy Current Displacement Sensor

Yuta Kawasaki and Hidetoshi Takahashi *

Department of Mechanical Engineering, Faculty of Science and Technology, Keio University, 3-14-1 Hiyoshi, Kouhoku-ku, Yokohama 223-8522, Japan
* Correspondence: htakahashi@mech.keio.ac.jp; Tel.: +81-45-566-1847

Abstract: This study proposes a force plate with a planar spring and an eddy current displacement sensor to measure the ground reaction force (GRF) of a small insect and reveal its motion characteristics. The proposed force plate comprises a circular aluminum plate, four aluminum springs symmetrically connected to the plate, and an eddy current displacement sensor under the plate. The diameter and thickness of the fabricated plate were 8 and 0.1 mm, respectively. The spring width was 0.4 mm. When a force is applied to the plate, the plate moves vertically downward. Then, an eddy current displacement sensor detects the plate displacement without contact. The applied force can be measured using Hooke's law. The proposed force plate has the advantages of ease of fabrication and cost-effectiveness. The central displacement variation and resonant frequency of the designed springs were evaluated by simulation. Then, we calibrated the fabricated force plate to obtain the sensitivity variation and resonant frequency. The experimental results suggest that the proposed force plate can effectively measure the GRF of a small insect.

Keywords: force plate; eddy current sensor; laser machining; ground reaction force; small insect

Citation: Kawasaki, Y.; Takahashi, H. Spiral Spring-Supported Force Plate with an External Eddy Current Displacement Sensor. *Actuators* **2023**, *12*, 16. https://doi.org/10.3390/act12010016

Academic Editor: Nicola Pio Belfiore

Received: 5 December 2022
Revised: 21 December 2022
Accepted: 29 December 2022
Published: 31 December 2022

1. Introduction

In the biomechanics field, ground reaction force (GRF) is an important factor in analyzing animal movement [1]. Force plates, consisting of a plate and force sensors under the plate, are generally used to measure GRF [2,3]. This type of force plate has been widely used for GRF in humans in sports science and rehabilitation [4–8]. In recent years, many researchers have developed a microelectromechanical system (MEMS)-based force plates to clarify the gait mechanism of small insects [9–19]. As small insects are less affected by gravity, they can run at high speeds on unstable footholds. Thus, GRF measurements and biomechanical evaluations are expected to aid in designing micro-running robots [20,21]. For example, a piezoresistive force plate with a size of a few square millimeters and a force resolution of approximately 1 μN was developed to measure the multi-axial GRF of an ant with body weight and length of a few milligrams and millimeters, respectively [22,23]. Although these MEMS force plates have high sensitivity, they are fragile, and the fabrication process is complex [24]. To achieve both high sensitivity and toughness, a plate structure with three-dimensional micro-springs was developed and manufactured using a precision 3D printer. Subsequently, by combining the plate structure and laser displacement sensor, a uniaxial force plate was assembled to measure the GRF of a fruit fly [25]. A force plate with sufficient performance for measuring small insects can be realized using this measurement principle.

Herein, we propose an unbreakable, easy-to-fabricate, and high-sensitivity force plate that consists of a planar spring and an eddy current displacement sensor under the planar spring. The planar spring installed in the proposed force plate comprises a circular plate and four planar springs. As this structure can be fabricated by cutting metal plates with a laser cutter machine, it is easier to fabricate than MEMS and 3D-printed force plates. Further, it is more accurate than 3D-printed force plates. The plate moves vertically downward when a force is applied to the planar spring. Unlike the measurement principle of MEMS force plates, the GRF is derived from the spring displacement measured using eddy current sensors, which are cost-effective when compared with a laser displacement sensor. This measurement principle does not require a large local strain, thus enabling an unbreakable design. Previously, we developed a force plate using a polyimide film-based planar spring and a laser displacement sensor [26]. The developed force plate realized a force resolution of less than 0.05 μN. Therefore, the planar spring geometry was confirmed to perform well as a force plate. Polyimide film deforms ductilely, which can cause hysteresis and affect measurement results. The previous study clarifies that force plates can be realized by using a laser displacement meter that measures a single point in the plate center.

In this study, we designed and fabricated a planar spring using a fiber-laser machine. The mechanical properties of the force plate were evaluated by simulation, and calibration and evaluation experiments were performed on the fabricated force plate.

2. Measurement System

Figure 1a shows the schematic of the proposed force plate. The proposed force plate comprises a planar spring and an eddy current displacement sensor with a planar coil. The planar spring moves downward when a vertical force is applied, as shown in Figure 1b. Then, the eddy current displacement sensor measures the plate displacement of the planar spring without making contact. The force applied can be calculated using Hooke's law from the displacement and spring constant. Specifically, force F is derived from the sensitivity K obtained by calibration and the sensor output change ΔV. Note that this relationship is based on the proportional relationship between the planar spring displacement and the sensor output and that the output is equal regardless of where the planar spring is pushed [25,26].

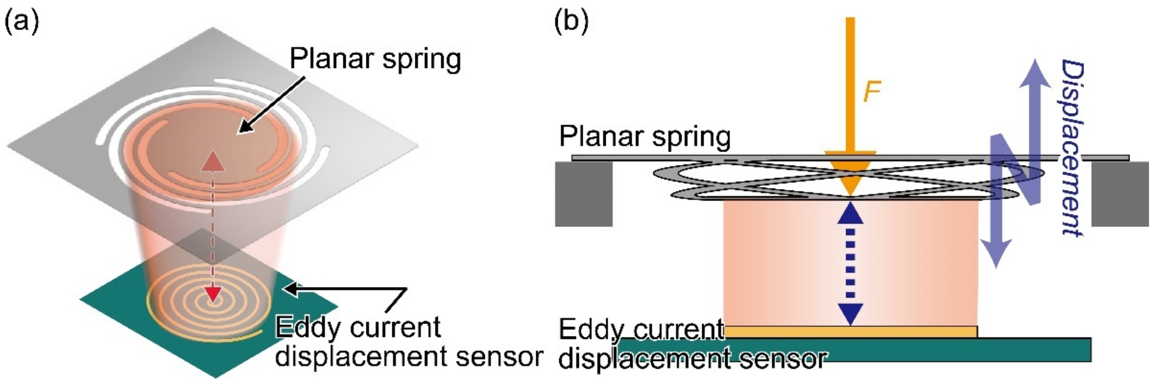

Figure 1. (**a**) Concept of the proposed force plate. This force plate consists of a planar spring and an eddy current displacement sensor. (**b**) Side view of the proposed force plate.

Previously, we developed a force plate for humans using multi-eddy current displacement sensor elements in the same way [27]. By using multiple sensor elements, multi-axial forces and moments were detected. On the contrary, the design guideline of this study is to accurately measure the uniaxial force using a single sensor element. Planar springs are suitable for measuring vertical force because a horizontal deformation does not tend to occur compared to that in 3D spring structures.

As shown in Figure 2, eddy currents are generated in the target metal when it moves due to the electromagnetic induction effect. This phenomenon changes the impedance of the planar coil. The sensor measures the distance based on the oscillation changes caused by this phenomenon. The insufficient size of the target metal or planar coil of the eddy current displacement sensor can cause a reduction in sensitivity. Therefore, the relationship between the size of the planar coil and the target metal should be appropriate. Aluminum is used as the target metal because of its high conductivity and ease of processing.

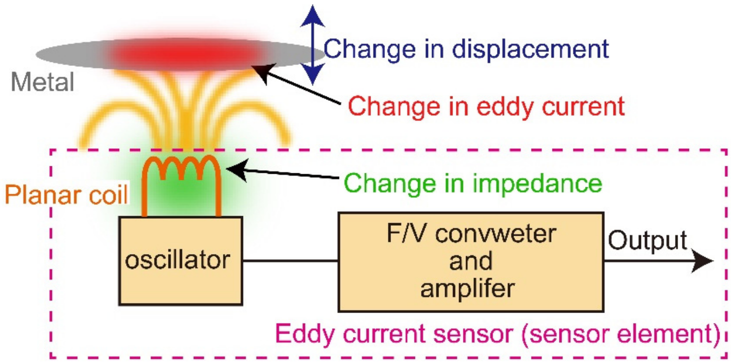

Figure 2. Schematic of the eddy current displacement sensor.

3. Design and Fabrication

3.1. Plate Structure

To measure the GRF of small insects, the plate area must range from a few to several tens of square millimeters. In addition, the force resolution needs to range from a few to dozens of micronewtons. The resonant frequency should be at least 100 Hz. These optimum requirements depend on the size and weight of the target insect.

Based on these requirements, we propose a force plate structure, as shown in Figure 3. This design is aimed at measuring the vertical GRF applied to the plate. The planar spring is composed of a circular plate with a diameter of 8 mm and four planar spring structures. The planar spring is 20 $\times$ 20 mm in size. The number of turns and thickness of the planar spring are 0.6 and 0.1 mm, respectively. The spring structures that support the center circular plate have a width of 0.4 mm and spacing of 0.6 mm between adjacent spring structures. As mentioned above, the planar spring is made of aluminum.

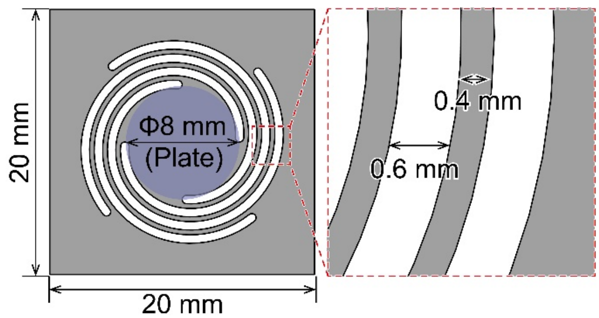

Figure 3. Detailed design of the planar spring.

All four spring structures supporting the central circular plate are similar and have the same spring constant k'. When a force is applied at a point, a reaction force is caused in the four springs, and a displacement occurs at the connection between the spring structure and the center circular plate. The displacement of the central circular plate is defined as z_0.

Based on the force-balancing relationship and Hooke's law, the following equation is valid:

$$F_0 = 4k'z_0. \tag{1}$$

From Equation (1), the GRF can be derived from the displacement of the center and spring constant, regardless of where the force is applied [26].

A simulation was conducted using finite element method (FEM) simulation software (COMSOL Multiphysics 6.0, COMSOL Inc, Burlington, VT, USA) to investigate whether the center displacements of the designed planar springs are the same when a vertical force of 1 mN is applied to points at any position. Figure 4(a-1,a-2) shows the deformation when a vertical force is applied. The smaller the displacement variation, the smaller the variation in the measured GRF, depending on the stepping position of the planar spring.

The simulation results are shown in Figure 4b. The inclination of the plate caused by applying a 1 mN force at the outermost point was 0.36°, which was adequately small to not interfere with the eddy current displacement sensor measurements. In this simulation, the center displacement variation was less than 0.1%, which was sufficiently small, and the average center displacement was 69.0 μm. The spring constant obtained from the central displacement when force was applied to the center was 14.5 N/m. Provided that the resolution of the displacement sensor is 1 μm, the resolution of the force plate can be calculated using the spring constant as 14.5 μN.

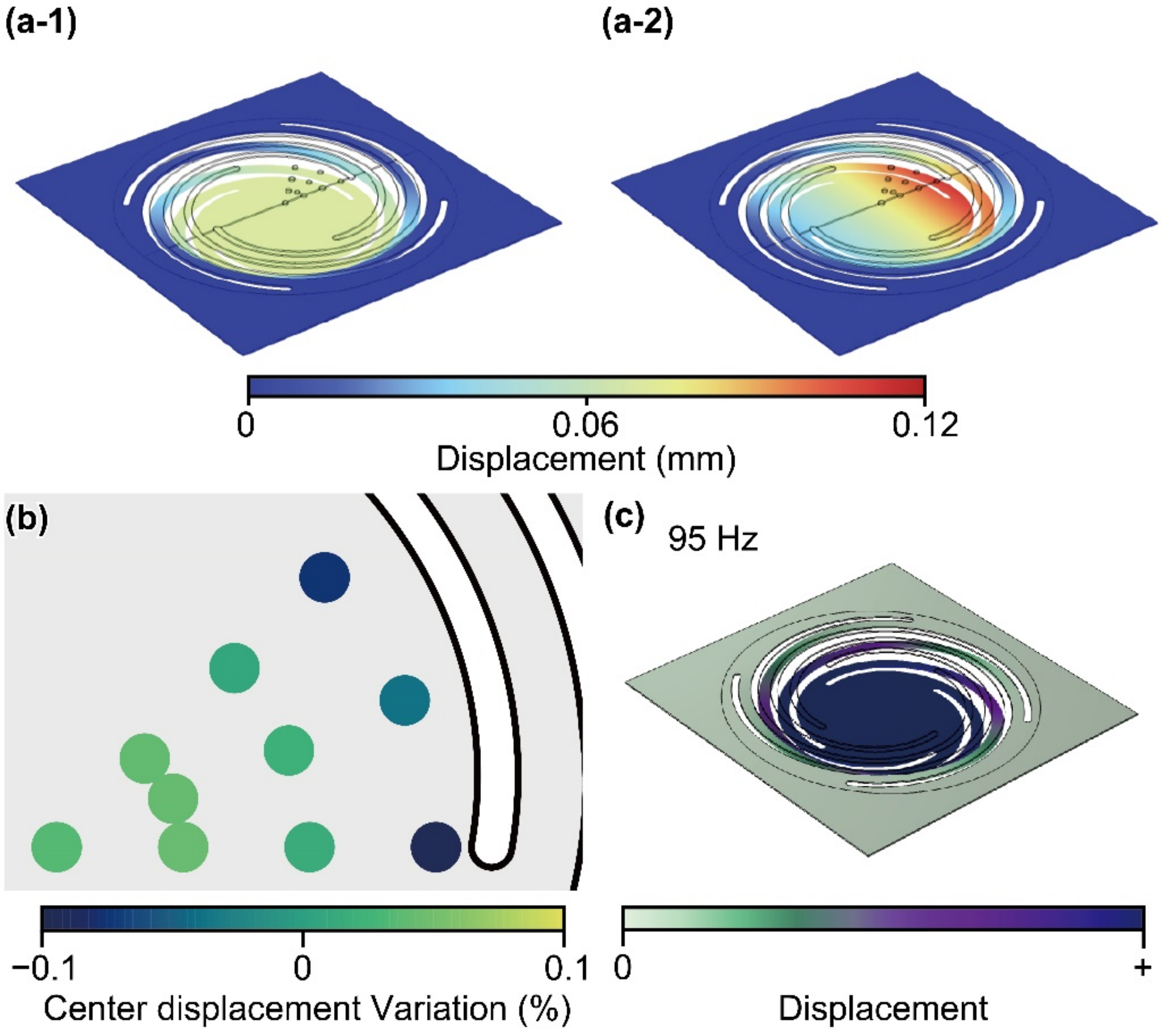

Figure 4. Simulation results of the deformation when a force is applied to (**a-1**) the center point and (**a-2**) the outermost point. (**b**) Spring constant variation determined from simulations. (**c**) Simulation result of the first resonant frequency.

In addition, the simulated resonant frequency was 95 Hz. Figure 4c shows the first mode of vibration.

The fabricated planar spring is illustrated in Figure 5a. This spring was made from an aluminum plate using a fiber laser cutting machine (PROMARK, PROFITED, Saitama, Japan) based only on 2D data from CAD. Thus, they can be fabricated more easily than MEMS force plates and more accurately than 3D-printed force plates. Figure 5b shows the force plate with the fabricated planar spring on the eddy current displacement sensor and the jig fabricated using a 3D printer (Onyx One, Markforged, Watertown, NY, USA).

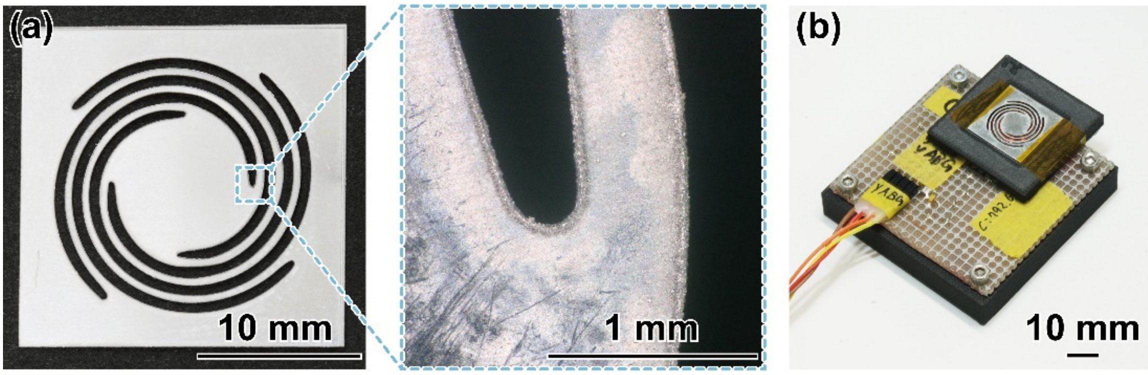

Figure 5. Photographs of (**a**) the fabricated planar spring by a fiber laser cutting machine and (**b**) the assembled force plate.

3.2. Eddy Current Displacement Sensor

Figure 6a shows the eddy current displacement sensor that can measure the metal displacement along with a planar coil with a diameter, resistance, and reactance of 10 mm, 1 Ω, and 8.4 μH, respectively. The size of the planar coil was chosen to be close to that of the central circular plate of the planar spring. Figure 6b shows that the planar coil is connected to the oscillator and square-wave generator circuits. An AC voltage of about 1 MHz is applied to the planar coil. The frequency of this square wave is converted into a voltage, which is the sensor output. This circuit uses a comparator (LT1671, LINEAR TECHNOLOGY, Wilmington, DE, USA). In+ and In− are input pins, and Q is the output. When the voltage of in+ is higher than In− (In+ > In−), Q outputs a high voltage, and when the converse occurs (In+ < In−), Q outputs a low voltage. Since In+, In−, and Q are connected by a feedback circuit, the output voltage of Q is a square wave. When the distance between the planar coil and the target metal changes, eddy currents flow in the target metal due to electromagnetic induction, changing the coil's impedance and frequency.

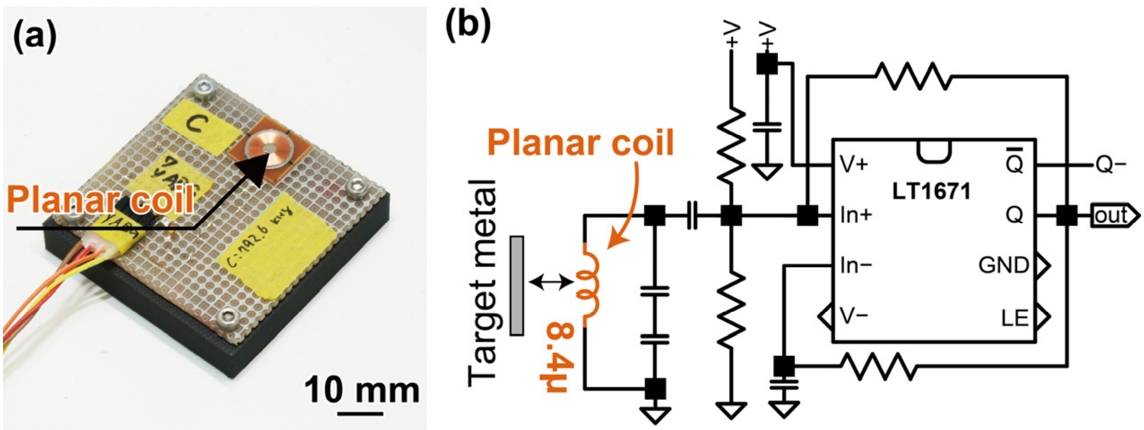

Figure 6. (**a**) Photograph of the eddy current displacement sensor. (**b**) Detailed design of sensor circuits.

The eddy current displacement sensor was calibrated, as shown in Figure 7a. In this study, the distance between the planar spring and the Al plate was 1 mm when no force was applied to the force plate. Therefore, the sensor output was measured when the distance was between 1 and 0.7 mm. The results are shown in Figure 7b. In this range, there is an approximately proportional relationship between the metal displacement and sensor output. The sampling rate was 2000 Hz, and a low-pass filter of 100 Hz was applied to the output. The resolution determined from the sensor output noise and sensitivity was 0.22 μm.

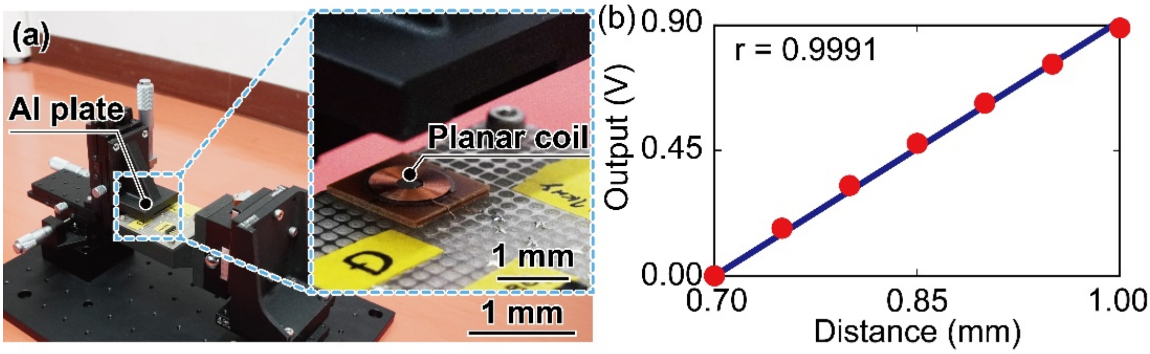

Figure 7. (**a**) Photograph of the experimental setup to calibrate the eddy current displacement sensor. (**b**) Relationship between the sensor output and the distance between the planar coil and Al plate.

4. Experiment and Result

4.1. Resonant Frequency

We measured the resonant frequency of the fabricated plate using an optical heterodyne (MLD-221 D-DWT, NEOARK, Hachioji, Japan) and a frequency response analyzer (NF, FRA5087). As shown in Figure 8a, the planar spring on the jig is mounted on a vibrator (Mini-shaker Type4810, Brüel and Kjær, Nærum, Denmark), applying vertical vibration to the planar spring from 10 to 200 Hz. Figure 8b shows the frequency response. It was confirmed that the first resonant frequency was 126 Hz, which was close to the simulation result and sufficiently high for GRF measurements.

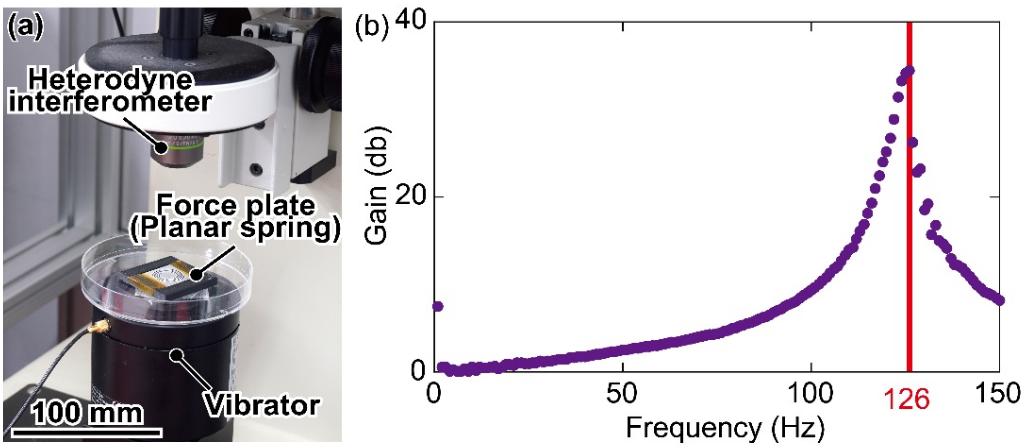

Figure 8. (**a**) Photograph of the experimental setup to evaluate the resonant frequency of planar spring. (**b**) Frequency response of the planar spring.

4.2. Evaluation of Sensitivity Variation and Calibration

Figure 9a,b shows the photograph and concept sketch of the experimental setup for evaluating the sensitivity variation and calibration, respectively. As shown in Figure 9c, 11 points (including the center and its surrounding points) were pushed using a needle mounted on a load cell (LVS-5GA, Kyowa Co., Chofu, Japan). The load cell was fixed on a piezo stage (PS1L60-400U-S; THK Precision Co., Ltd., Ota-ku, Tokyo, Japan). The stage displacement was controlled with a triangular wave of 0.2 Hz. The center and its surrounding points, within a quarter of the area, were considered for symmetry. The piezo stage was moved up and down by 0.1 mm, and the needle mounted to the load cell applied a vertical force to the planar spring. The stage displacement, applied force, and output of the displacement sensor was measured simultaneously.

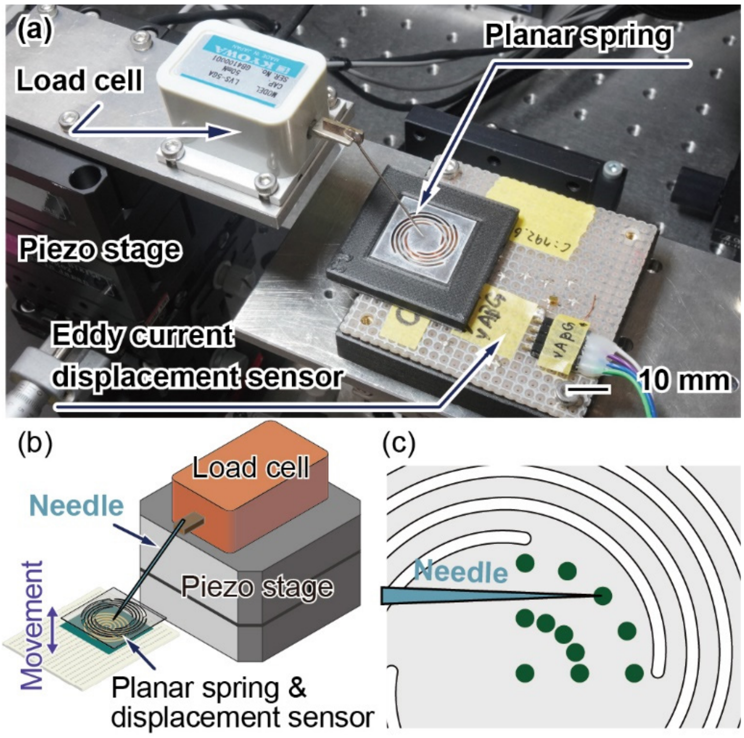

Figure 9. (**a**) Photograph and (**b**) concept sketch of the experimental setup for calibration and evaluation of sensitivity variation. (**c**) 11 points pushed on the planar spring.

Figure 10 shows the displacement of the piezo stage Z_{stage}, force applied by the load cell F, and force plate output (eddy current displacement sensor output) V_{FP}. When the piezo stage was at its highest, no force was applied to the force plate to obtain the zero point of the V_{FP}. When the piezo stage was at its lowest, a force of approximately 2.5 mN was applied. It was observed that there was no hysteresis in the force plate output.

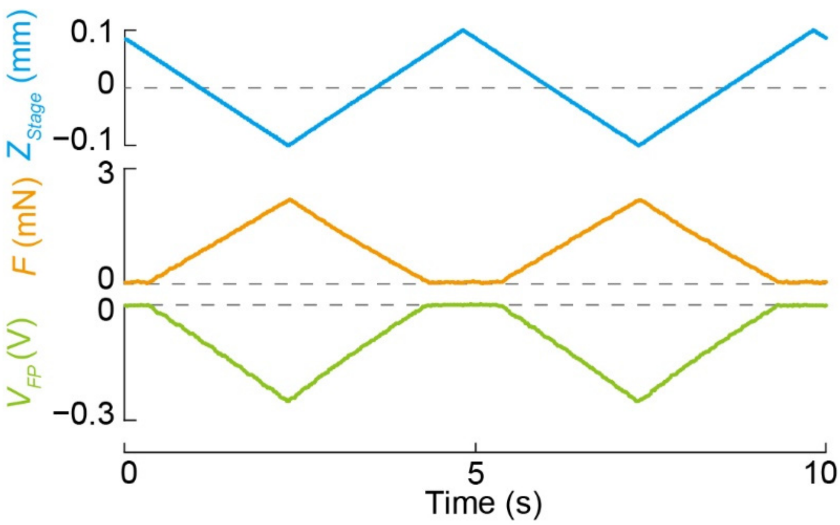

Figure 10. Measured Z_{stage}, F, and V_{FP} when the needle was pushing at the center.

Figure 11 shows the relationship between F and V_{FP} when each point was pushed. The correlation coefficient was between 0.999 and 1.000, and we confirmed a good linear relationship between the force and force plate output; this is considered to be due to the spring stress being within aluminum's elastic range. Therefore, Equation (1) can be applied.

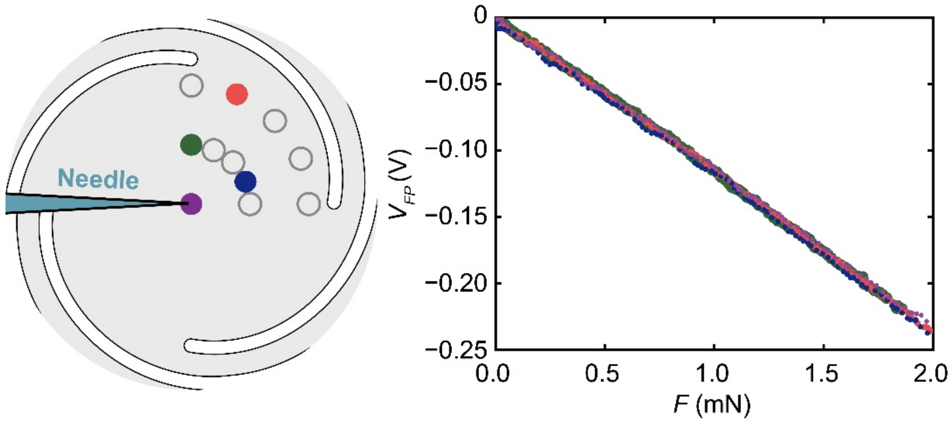

Figure 11. Some examples of the relationship between F and V_{FP}. The color of each point in the left diagram corresponds to the color in the right graph.

When a planar spring is pushed by the needle connected to the load cell, displacement occurs in the planar spring as well as on the load cell side; moreover, displacement occurs in the opposite direction of the planar spring owing to the reaction force. Therefore, Z_{stage} is the sum of the displacements at the pushed point (Z_{sp}) and load cell ($Z_{load\text{-}cell}$). $Z_{load\text{-}cell}$ was obtained from the measurement results when the hard part was pushed, and the spring constant of the load cell was derived. Therefore, Z_{sp} can be evaluated by subtracting $Z_{load\text{-}cell}$ from Z_{stage}. The spring constant of the planar spring was 15.5 N/m when a force was applied at the center, which was evaluated using F and Z_{sp}.

The sensitivity was evaluated using a gradient of F and V_{FP}. Figure 12 shows the sensitivity variation, which was less than 3.0%; this was considered sufficiently small. The average sensitivity K was −8.52 mN/V. No trend was observed in the sensitivity variation. Therefore, this variation is not attributed to the design, but to assembly and experimental setup errors. The sampling rate was 5000 Hz, and a low-pass filter of 100 Hz was applied to the output. If the signal when no force was applied to the force plate was at the noise level, the noise level was 1.19 mV. The noise was assumed to be caused by environmental vibrations. The force resolution was calculated to be 4.14 µN. MEMS-based Force plates for ants with a resolution of a few micronewtons have been reported, and it is thought that ant GRF can be measured with our force plate [11].

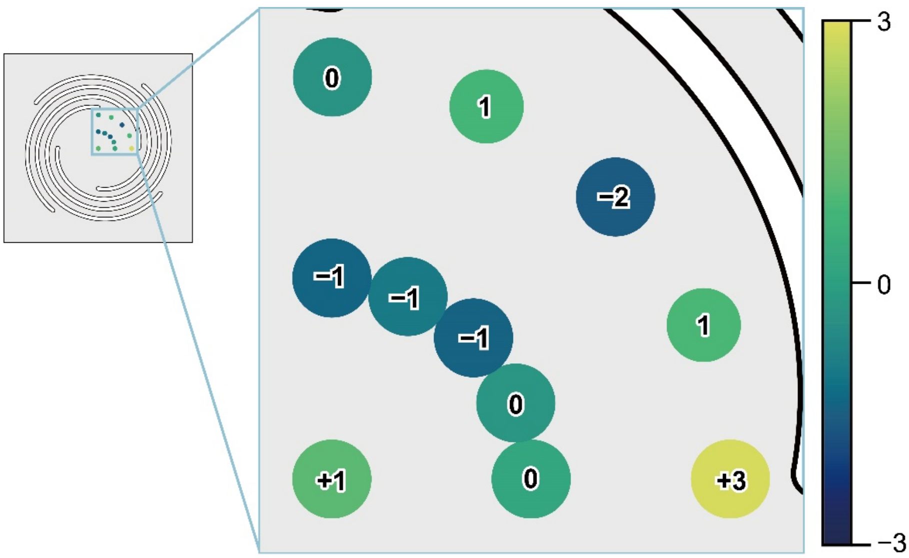

Figure 12. Sensitivity variation obtained by the experiments.

4.3. Repeatable and Durable Tests

Pushing the center for one hour under the same experimental conditions in Section 4.2. The maximum value of F is approximately 25 mN. The waveform shapes of V_{FP} and F did not change as shown in Figure 13. Therefore, the fabricated force plate is considered to have sufficient repeatability and durability.

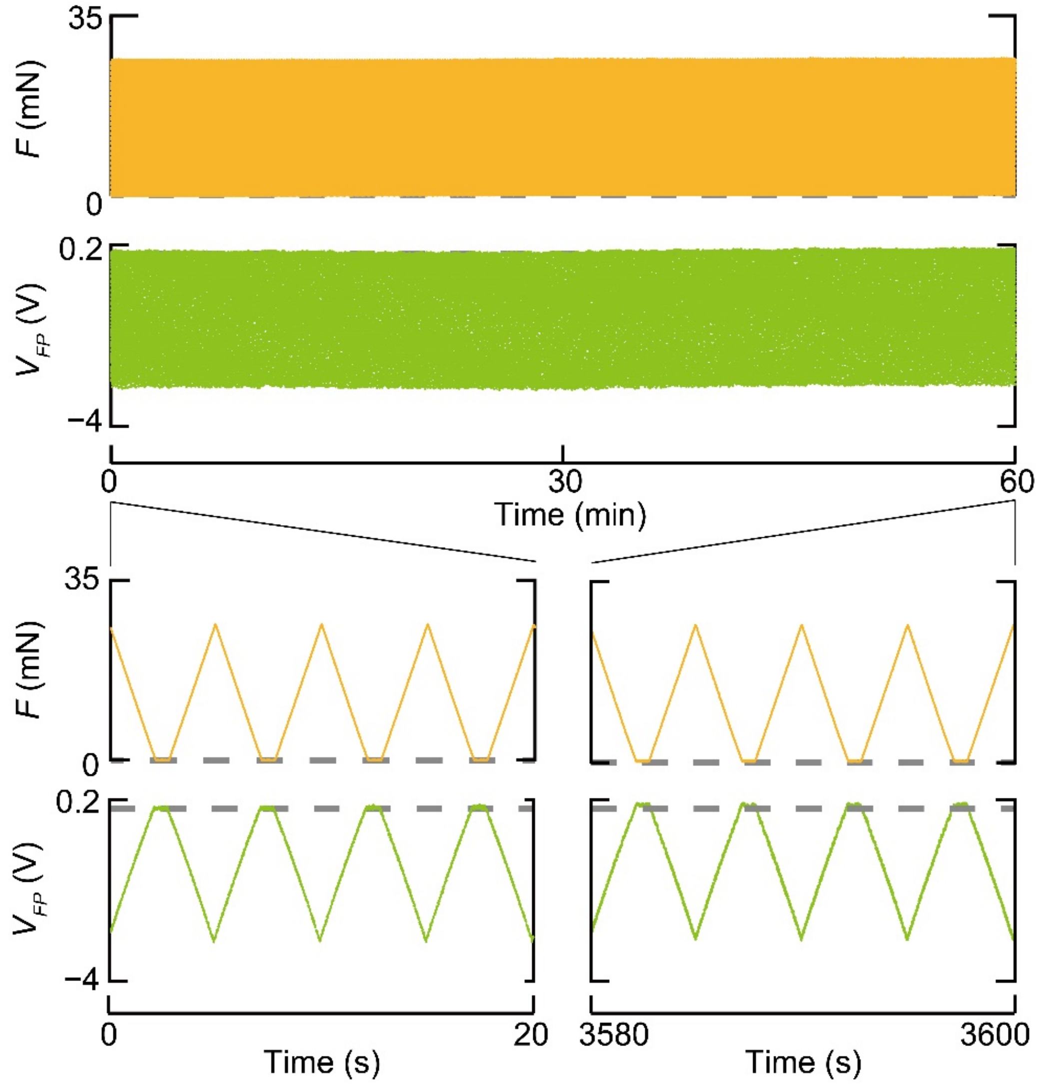

Figure 13. Measured F and V_{FP} when the needle was pushed at the center for one hour.

5. Discussion

The proposed force plate was fabricated using simple fabrication processes. It was confirmed that the force plate could measure forces similar to the GRF of small insects.

The planar spring design significantly influences the overall performance in terms of the maximum load, resolution, and resonant frequency. Therefore, smaller or larger forces can be measured by changing the planar spring design. For example, in the design used in this study, a smaller force can be measured if the width of the spring structure supporting the central circular plate is smaller than the current design. However, this change can reduce the maximum load and resonant frequency of the planar spring. The fiber laser cutting machine can process planar springs in various designs; however, the limitation is that the design is point-symmetric. Therefore, we can better optimize the design of planar springs for our target insects.

In this study, aluminum was used as the planar spring material. The material type is limited to metals that can be measured by eddy current displacement sensors. However, the physical properties of the planar spring material and its design have a significant influence on the performance of the force plate. In particular, the stiffness and toughness significantly influence the durability and sensitivity of the force plate.

When designing force plates, there is a trade-off between force resolution and force range in general. In this study, the width of the planar spring structure was 4 mm, and the resolution was approximately 4 μN, which was within the range for ant measurement. A design of a softer planar spring would result in a force plate with a higher sensitivity and a smaller force range. Additionally, as a small non-contact displacement sensor, eddy current displacement sensors with a full-scale range of 3 mm have been reported [28,29]. These sensors had a resolution of 3 μm and an excitation frequency of 312.5 kHz [28] or a resolution of 65 nm and an excitation frequency of 20 MHz [29]. These state-of-the-art eddy current displacement sensors suggested that it is possible to improve the performance of our force plate.

In actual GRF measurement, mechanical property changes of the planar spring due to temperature changes may lead to measurement uncertainty. The measurements should be carried out under stable temperatures to avoid temperature effects on small insects' movement. Since GRF measurement and calibration can be conducted in the same environment, the influence of temperature changes on the sensor is expected to be negligible in GRF measurement. Additionally, the previous study mentioned noise due to jigs and thermal expansion of other mechanical parts [25]. This was because the force plate and non-contact displacement sensor had to be fixed by large jigs and xyz stage compared to the force plate. However, the proposed force plate consists of the eddy current displacement sensor, planar spring, and small jig, and the effect of thermal expansion of the jig is considered sufficiently small.

This study aimed to measure only the vertical forces. By measuring multi-axial deformations, the force plate is expected to measure the GRF in multi-axial directions [27]. In previous studies, multi-axial displacements were measured by arranging multiple planar coils in the same plane, as the measurement target of eddy current displacement sensors is only metal [13]. Therefore, eddy current displacement sensors are expected to be used in developing force plates that can measure multi-axial deformations via simple approaches.

6. Conclusions

This study proposed a force plate comprising a planar spring and an eddy current displacement sensor. Planar springs are obtained by laser-cutting an Al plate. Therefore, they are easier to fabricate than MEMS-based force plates. The proposed GRF measurement principle minimizes the smaller local strains. Thus, a force plate with higher toughness can be designed. The FEM simulation confirmed that the resonant frequency of the designed force plate was 95 Hz, and the spring-constant variation was less than 0.1%. Further, the resonant frequency and sensitivity variation of the fabricated force plates were determined as 126 Hz and less than 3%, respectively, via evaluation experiments. Therefore, the proposed force plate enables easy fabrication and higher toughness and is significant in the GRF evaluation of small insects.

Author Contributions: H.T. conceptualized and supervised the study, and Y.K. designed and developed the force plate and performed the calibration experiment. Y.K. and H.T. analyzed the measurement data and wrote the paper. All authors have read and agreed to the published version of the manuscript.

Funding: This research was partly supported by JSPS KAKENHI Grant No. 20K20984 and the Shi-madzu Science Foundation.

Institutional Review Board Statement: Not applicable.

Informed Consent Statement: Not applicable.

Data Availability Statement: The data presented in this study are available on request from the corresponding author.

Acknowledgments: The authors thank Takashi Nakamura for developing the measurement circuit.

Conflicts of Interest: The authors declare no conflict of interest.

References

1. Dickinson, M.H.; Farley, C.T.; Full, R.J.; Koehl, M.A.R.; Kram, R.; Lehman, S. How Animals Move: An Integrative View. *Science* **2000**, *288*, 100–106. [CrossRef] [PubMed]
2. Ferryanto, F.; Akbar, M.M.; Wicaksono, S.; Mahyuddin, A.I. Design, Manufacture, and Testing of a Low-Cost Force Platform with 3-Axis Load Cell. *IOP Conf. Ser. Mater. Sci. Eng.* **2021**, *1109*, 012021. [CrossRef]
3. Silva, M.G.; Moreira, P.V.S.; Rocha, H.M. Development of a Low Cost Force Platform for Biomechanical Parameters Analysis. *Res. Biomed. Eng.* **2017**, *33*, 259–268. [CrossRef]
4. Liikavainio, T.; Isolehto, J.; Helminen, H.J.; Perttunen, J.; Lepola, V.; Kiviranta, I.; Arokoski, J.P.A.; Komi, P.V. Loading and Gait Symmetry during Level and Stair Walking in Asymptomatic Subjects with Knee Osteoarthritis: Importance of Quadriceps Femoris in Reducing Impact Force during Heel Strike? *Knee* **2007**, *14*, 231–238. [CrossRef] [PubMed]
5. Ogawa, A.; Iijima, H.; Takahashi, M. Staircase Design for Health Monitoring in Elderly People. *J. Build. Eng.* **2021**, *37*, 102152. [CrossRef]
6. Schieb, D.A. The force plate in sports biomechanics research. In Proceedings of the 4 International Symposium on Biomechanics in Sports, Halifax, NS, Canada, 15–19 July 1986; pp. 337–365.
7. Goble, D.J.; Manyak, K.A.; Abdenour, T.E.; Rauh, M.J.; Baweja, H.S. An Initial Evaluation of the Btracks Balance Plate and Sports Balance Software for Concussion Diagnosis. *Int. J. Sports Phys. Ther.* **2016**, *11*, 149–155.
8. Hrysomallis, C. Relationship between Balance Ability, Training and Sports Injury Risk. *Sport. Med.* **2007**, *37*, 547–556. [CrossRef]
9. Kohyama, S.; Takahashi, H.; Takahata, T.; Shimoyama, I. High Sensitive and Large Area Force Plate for Ground Reaction Force Measurement of Ant Running. In Proceedings of the 2018 IEEE Micro Electro Mechanical Systems (MEMS), Belfast, UK, 21–25 January 2018; pp. 874–877. [CrossRef]
10. Sun, Y.; Potasek, D.P.; Fry, S.N.; Nelson, B.J. Characterizing Fruit Fly Flight Behavior Using a Micro Force Sensor with a New Comb Drive Configuration. *Proc. IEEE Int. Conf. Micro Electro Mech. Syst.* **2004**, *14*, 837–840. [CrossRef]
11. Takahashi, H. MEMS-Based Micro Sensors for Measuring the Tiny Forces Acting on Insects. *Sensors* **2022**, *22*, 8018. [CrossRef]
12. Furuya, R.; Takahashi, T.; Vinh, N.T.; Yano, T.; Ito, K.; Takahata, T.; Matsumoto, K.; Shimoyama, I. Measurement of jumping force of a fruit fly using a mesa structure force plate. In Proceedings of the 2016 IEEE 29th International Conference on Micro Electro Mechanical Systems (MEMS), Shanghai, China, 24–28 January 2016; pp. 165–168. [CrossRef]
13. Wang, L.; Jones, D.; Chapman, G.J.; Siddle, H.J.; Russell, D.A.; Alazmani, A.; Culmer, P. An Inductive Force Sensor for In-Shoe Plantar Normal and Shear Load Measurement. *IEEE Sens. J.* **2020**, *20*, 13318–13331. [CrossRef]
14. Reinhardt, L.; Blickhan, R. Level Locomotion in Wood Ants: Evidence for Grounded Running. *J. Exp. Biol.* **2014**, *217*, 2358–2370. [CrossRef] [PubMed]
15. Bartsch, M.S.; Federle, W.; Full, R.J.; Kenny, T.W. A Multiaxis Force Sensor for the Study of Insect Biomechanics. *J. Microelectromech. Syst.* **2007**, *16*, 709–718. [CrossRef]
16. Full, R.J.; Tu, M.S. Mechanics of a Rapid Running Insect: Two-, Four- and Six-Legged Locomotion. *J. Exp. Biol.* **1991**, *156*, 215–231. [CrossRef] [PubMed]
17. Full, R.J.; Blickhan, R.; Ting, L.H. Leg Design in Hexapedal Runners. *J. Exp. Biol.* **1991**, *158*, 369–390. [CrossRef] [PubMed]
18. Full, R.J.; Tu, M.S. Mechanics of Six-Legged Runners. *J. Exp. Biol.* **1990**, *148*, 129–146. [CrossRef] [PubMed]
19. Reinhardt, L.; Blickhan, R. Ultra-Miniature Force Plate for Measuring Triaxial Forces in the Micronewton Range. *J. Exp. Biol.* **2014**, *217*, 704–710. [CrossRef] [PubMed]
20. Wu, Y.; Yim, J.K.; Liang, J.; Shao, Z.; Qi, M.; Zhong, J.; Luo, Z.; Yan, X.; Zhang, M.; Wang, X.; et al. Insect-Scale Fast Moving and Ultrarobust Soft Robot. *Sci. Robot.* **2019**, *4*, eaax1594. [CrossRef]
21. Kevin, Y.M.; Pakpong, C.; Sawyer, B.; Fuller, J.W.; Robert, J.W. Controlled Flight of a Biologically Inspired, Insect-Scale Robot. *Science* **2013**, *340*, 603–607. [CrossRef]
22. Endlein, T.; Federle, W. On Heels and Toes: How Ants Climb with Adhesive Pads and Tarsal Friction Hair Arrays. *PLoS ONE* **2015**, *10*, e0141269. [CrossRef]
23. Takahashi, H.; Thanh-Vinh, N.; Jung, U.G.; Matsumoto, K.; Shimoyama, I. MEMS Two-Axis Force Plate Array Used to Measure the Ground Reaction Forces during the Running Motion of an Ant. *J. Micromech. Microeng.* **2014**, *24*, 065014. [CrossRef]
24. Tkahashi, H.; Furuya, R.; Yano, T.; Takahata, T.; Shimoyama, I. Maximum force capacity of legs of a fruit fly during landing motion. In Proceedings of the International Conference on Solid-State Sensors, Actuators and Microsystems (TRANSDUCERS), Kaohsiung, Taiwan, 18–22 June 2017; pp. 1061–1064. [CrossRef]
25. Sugimoto, T.; Kawasaki, Y.; Toda, H.; Takahashi, H. Measurement Method of a Microspring-Supported Force Plate with an External Laser Displacement Meter. *Meas. Sci. Technol.* **2022**, *33*, 105118. [CrossRef]
26. Shimazaki, K.; Sugimoto, T.; Toda, H.; Takahashi, H. A Polyimide Film-Based Simple Force Plate for Measuring the Body Mass of Tiny Insects. *Sensors* **2022**, *22*, 8352. [CrossRef] [PubMed]

27. Kawasaki, Y.; Ogawa, A.; Takahashi, H. Force Plate with Simple Mechanical Springs and Separated Noncontact Sensor Elements. *Sensors* **2021**, *21*, 7092. [CrossRef] [PubMed]
28. Oberle, M.; Reutemann, R.; Hertle, J.; Huang, Q. A 10-MW Two-Channel Fully Integrated System-on-Chip for Eddy-Current Position Sensing. *IEEE J. Solid-State Circuits* **2002**, *37*, 916–925. [CrossRef]
29. Nabavi, M.R.; Pertijs, M.A.P.; Nihtianov, S. An Interface for Eddy-Current Displacement Sensors with 15-Bit Resolution and 20 Mhz Excitation. *IEEE J. Solid-State Circuits* **2013**, *48*, 2868–2881. [CrossRef]